Altering Hydrogen Storage Properties by Hydride Destabilization through Alloy Formation: LiH and MgH_2 Destabilized with Si

John J. Vajo*

HRL Laboratories, LLC, 3011 Malibu Canyon Road, Malibu, California 90265

Florian Mertens

General Motors Research and Development Center, 30500 Mound Road, Warren, Michigan 48090

Channing C. Ahn, Robert C. Bowman, Jr.,† and Brent Fultz

Division of Engineering and Applied Science, California Institute of Technology, Pasadena, California 91125

Received: January 26, 2004; In Final Form: May 17, 2004

Alloying with Si is shown to destabilize the strongly bound hydrides LiH and MgH_2. For the LiH/Si system, a $Li_{2.35}Si$ alloy forms upon dehydrogenation, causing the equilibrium hydrogen pressure at 490 °C to increase from approximately 5×10^{-5} to 1 bar. For the MgH_2/Si system, Mg_2Si forms upon dehydrogenation, causing the equilibrium pressure at 300 °C to increase from 1.8 to >7.5 bar. Thermodynamic calculations indicate equilibrium pressures of 1 bar at approximately 20 °C and 100 bar at approximately 150 °C. These conditions indicate that the MgH_2/Si system, which has a hydrogen capacity of 5.0 wt %, could be practical for hydrogen storage at reduced temperatures. The LiH/Si system is reversible and can be cycled without degradation. Absorption/desorption isotherms, obtained at 400−500 °C, exhibited two distinct flat plateaus with little hysteresis. The plateaus correspond to formation and decomposition of various Li silicides. The MgH_2/Si system was not readily reversible. Hydrogenation of Mg_2Si appears to be kinetically limited because of the relatively low temperature, <150 °C, required for hydrogenation at 100 bar. These two alloy systems show how hydride destabilization through alloy formation upon dehydrogenation can be used to design and control equilibrium pressures of strongly bound hydrides.

1. Introduction

A commercially viable hydrogen storage technology is one of the major obstacles to the widespread use of fuel cells for transportation applications. In addition to safety and reliability, high volumetric and gravimetric storage densities are needed.[1,2] System-based densities of at least 62 kg/m^3 and 6.5 wt % hydrogen are desired.[3,4] The stored hydrogen should be recoverable and preferably rechargeable on-board at temperatures of <100−200 °C with pressures below approximately 100 bar.

Hydrogen may be stored in molecular form as a liquid or compressed gas, or it may be adsorbed on a suitable support. Liquefaction consumes 30% of the energy content of the stored hydrogen, and liquid hydrogen can be difficult to maintain for extended times without significant loss. Compression also requires energy input, and acceptable storage densities require pressures in excess of 350 bar, which pose engineering challenges. Molecular adsorption can partially alleviate the extreme pressures and temperatures associated with liquefied and compressed hydrogen. However, because H_2 is nonpolar and contains only two strongly covalently bound electrons, electrostatic and dispersive bonds to adsorbents are weak. The best current materials, high surface area activated carbons, still require cryogenic temperatures to achieve high (5.5 wt %) storage densities.[5,6] Nanostructured carbons, including single-wall carbon nanotubes, while promising because of their structural and chemical versatility, have not consistently shown superior hydrogen storage properties.[7−11]

Hydrogen can also be stored chemically in the form of atoms, cations (protons), or hydride anions. The interaction of hydrogen with transition-metal elements and alloys has been studied extensively.[12−15] However, stoichiometries generally do not exceed two hydrogen atoms per metal atom, which largely precludes transition metals from achieving gravimetric densities of >5 wt %. Typical values are 1−3 wt %. Recently, salts of the complex hydride anion $[AlH_4]^-$ have received attention since the discovery that with Ti as a catalyst or dopant, three-fourths of the hydrogen in $NaAlH_4$ (5.6 wt %) can be stored reversibly.[16−18] A reversible transformation of $LiNH_2 + LiH$ to Li_2NH, which theoretically stores 6.4 wt % hydrogen, has also been described.[19,20] Hydrides of many period 2 and 3 elements are known to have relatively high, >5 wt %, hydrogen densities. However, most of these hydrides are very stable and do not release hydrogen until the temperature exceeds 250 °C. Two examples are LiH and MgH_2. Lithium hydride contains 12.5 wt % hydrogen, but requires 910 °C for an equilibrium pressure of 1 bar.[21] Magnesium hydride contains 7.7 wt % hydrogen and has a 1 bar equilibrium pressure at 275 °C.[15]

Because of its stability, LiH has not been considered a practical hydrogen storage material. Magnesium hydride, although more stable than desired for most applications, has been studied in detail.[22,23] Many of these studies have focused on

* Corresponding author. E-mail: vajo@hrl.com.
† Also at: Jet Propulsion Laboratory, California Institute of Technology, Pasadena, CA 91109.

10.1021/jp040060h CCC: $27.50
Published on Web 08/19/2004

processing, such as mechanical milling,[22,24,25] and additives that might improve reaction kinetics and increase equilibrium pressures. The objectives of many processing studies have been to improve diffusion rates by, for example, reducing the particle size, minimizing diffusion distances, and introducing defects. Studies of additives have been directed at catalyzing the absorption and desorption of hydrogen. Both processing and additives have produced considerable improvement in the kinetics.[22,24] However, in almost all studies, equilibrium pressures, or more generally the thermodynamics of the interaction of hydrogen with Mg, have remained virtually unchanged.[25]

Since the pioneering work of Reilly,[26,27] modification of hydrogenation/dehydrogenation thermodynamics has been accomplished using additives that form alloys or compounds with Mg in either or both the hydrogenated or dehydrogenated states.[28,29] A well-known example is Mg_2Ni, which, upon hydrogenation, forms Mg_2NiH_4 with 3.6 wt % hydrogen and an equilibrium pressure of 1 bar at 245 °C.[15,30] Aluminum has been found to destabilize MgH_2 by forming a Mg/Al alloy upon dehydrogenation.[28] The reaction is reversible with MgH_2 and Al reforming and segregating during hydrogenation. At 280 °C, the equilibrium pressure is a factor of 3 larger than that of pure MgH_2.

To address the low equilibrium pressure in strongly bound hydride systems we also have considered additives that form compounds or alloys with the dehydrogenated metals. If a compound is stable with respect to its constituent elements, then the hydride will be effectively destabilized. Destabilization occurs because the system can cycle between the hydride and the compound instead of the elemental metal. In this work, we use Si to destabilize Li and Mg hydrides. Silicon forms relatively strongly bound compounds with Li and Mg that reduce dehydrogenation enthalpies and increase equilibrium hydrogen pressures.

2. Experimental Procedures

Lithium hydride (95% purity from Aldrich and 97% purity from Fluka) and MgH_2 (95% purity from Gelest) were used without further purification. Pieces of Si were cleaved from electronic-grade Si wafers. All sample handling was performed in an Ar-filled glovebox. Mixtures of LiH + Si and MgH_2 + Si were prepared using mechanical milling. Approximately 1 g of mixtures were milled with a Fritsch Pulversette 6 planetary mill at 400 rpm for 1 h in an 80-cm^3 hardened steel vessel with 30 7-mm diameter chrome−steel balls. This mixing period is much shorter than the 2−80 h of mechanical milling that have been commonly used to produce nanocrystalline and amorphous phases in magnesium alloys and hydrides.[22,28,30]

Temperature ramp dehydrogenation/hydrogenation and isotherm measurements were performed in two custom Sieverts' apparatus. The temperature ramp experiments were performed using an all-metal stainless steel system employing welded and metal gasket couplings. The system was pumped using an oil-free pumping station (Tribodyn 100/120-HVP, Danielson Associates). A base pressure at the pump inlet of $<1 \times 10^{-8}$ Torr (1.3×10^{-6} Pa) was routinely obtained. The pressure at the sample, which was separated from the pump by approximately 1 m of 0.953-cm outside-diameter tubing, several valves, and a 2-μm filter gasket, was measured by replacing the sample container with an ionization gauge. After being pumped overnight, a pressure of 1×10^{-6} Torr (1.3×10^{-4} Pa) was obtained. Hydrogen pressures were measured using low-range (0−100 psia) and high-range (0−3000 psia) capacitance manometers (model 216FSF, Setra Systems, Inc.). Gas temperatures were measured with thermocouples spot-welded to the system. Sample temperatures were measured with a thermocouple inside a thermowell in the sample container. The sample container was heated using a cylindrical band heater immersed in a glass dewar filled with 2-mm diameter glass beads. Pressures and temperatures were recorded by computer using LabView software. Approximately 0.7−0.9 g of the milled mixtures were used and typically evacuated overnight. Samples were desorbed into volumes of 220 cm^3 for the Li/Si experiments and 60 cm^3 for the Mg/Si experiments. Only a small volume of 20 cm^3 containing the samples was heated. After desorption, the composition of desorbed gas was monitored using a residual gas analyzer connected to the desorption volume through a leak valve. Hydrogenation measurements were conducted using an initial hydrogen pressure of 100 bar in a volume of 60 cm^3. The hydrogen had a purity of 99.9995% and was used without further purification. After loading into the system, the temperature and pressure were equilibrated for at least 1 h.

The isotherm measurements were performed using an all-metal Sieverts volumetric system constructed from electropolished 316L stainless steel tubing and components. The system, consisting of a central manifold (50 cm^3), an extension to the sample (20 cm^3), two reference volumes (150 and 1000 cm^3), and a sample container (8 cm^3), was assembled using a combination of orbital welding and various metal-to-metal interface seals to connect valves and pressure sensors. An integrated vacuum station (model RS-200, HOVAC, Inc.) consisting of an oil-free diaphragm and molecular drag pump was used to attain pressures below 2×10^{-7} Torr (2.7×10^{-5} Pa) at the pump inlet. A high-accuracy capacitance manometer system (models 120AA/510B combination, MKS Instruments) was used for pressure measurements. Research grade hydrogen gas was flowed through a point-of-use chemical filter (Millipore Corporation) prior to entering the Sieverts manifold and reference volumes. The stainless steel sample container was fully immersed into a fluidized sand bath (Techne, Inc.) that was controlled to ± 1−2 °C at selected temperatures over the range from 75 to 575 °C. Calibrated platinum resistance thermometers were bonded to external surfaces of the manifold and reference volumes while sheathed type-K thermocouples were attached at three locations on the exterior of the sample container. A computer operating with LabView software controlled a series of pneumatic valves to expose the sample to vacuum, gas supply, or reference volumes as needed in addition to performing data collection and processing during automated isotherm measurements.

X-ray data were obtained with a Philips PW3040-Pro diffractometer using Cu Kα radiation and an X-ray mirror. Samples were mounted into 1-mm glass capillary tubes in an Ar glovebox and sealed prior to data acquisition. The capillary contribution to the diffraction data was subtracted from each of the traces.

3. Results

Dehydrogenation and rehydrogenation of LiH/Si mixtures during temperature ramps are shown in Figure 1a and b, respectively. Figure 1a shows dehydrogenation of a mixture with the stoichiometry 4LiH + Si and, for comparison, a similarly milled sample of pure LiH. Hydrogen desorption from this LiH/Si mixture begins at approximately 270 °C and reaches 0.78 wt %. Given the sample mass and desorption volume, 0.78 wt % desorption occurs at 0.4 bar, which is the equilibrium pressure at 450 °C for the LiH/Si system. In contrast, the sample of LiH

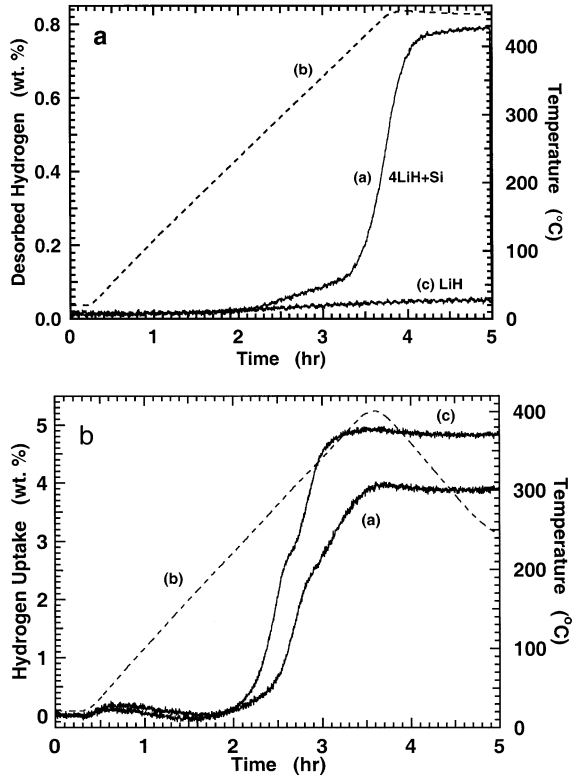

Figure 1. Dehydrogenation and rehydrogenation in the LiH/Si system. (a) Hydrogen desorption from milled LiH and 4LiH + Si. Curves a and b show the wt % and temperature, respectively, during heating 4LiH + Si at 2 °C/min to 450 °C. Hydrogen desorption begins at approximately 270 °C and accelerates at approximately 380 °C. Beyond 4.2 h, the amount of desorbed hydrogen becomes constant at 0.78 wt %, corresponding to a pressure of 0.4 bar. Curve c shows the wt % hydrogen during heating of pure LiH. As expected, no hydrogen desorption occurs in this temperature range. (b) Hydrogenation of dehydrogenated milled LiH/Si mixtures. Curves a and b show the wt % hydrogen uptake and temperature, respectively, during heating and cooling of a vacuum dehydrogenated 4LiH + Si mixture in, initially, 100 bar of hydrogen. The mixture was initially dehydrogenated by heating under vacuum to 450 °C for 3 h. Hydrogen uptake begins at approximately 230 °C and reaches 3.9 ± 0.1 wt %. Curve c shows the hydrogen uptake for 2.5LiH + Si; in this case the uptake reaches 4.9 ± 0.1 wt %. The S-shaped behavior of the uptake curves at the start of heating and the slight decline upon cooling are instrumental artifacts due to imperfect accounting for gas heating.

milled without Si showed no hydrogen desorption in this temperature range. Figure 1b shows rehydrogenation of LiH/Si mixtures dehydrogenated under vacuum at 450 °C for 3 h. Vacuum pressure measurements indicated that the flux of hydrogen diminished considerably after 1 h at 450 °C. Hydrogen uptake from an initial pressure of 100 bar begins at approximately 230 °C, and for a 4LiH + Si mixture it reaches 3.9 ± 0.1 wt %. This hydrogen uptake suggests that the silicide formed during dehydrogenation had the composition $Li_{2.3}Si$, not Li_4Si as given by the mixture stoichiometry. The X-ray data presented below confirm this composition. If $Li_{2.3}Si$ is the limiting dehydrogenated composition, then an initial mixture of 2.3LiH + Si should yield 5.0 wt % hydrogen uptake after dehydrogenation. As also shown in Figure 1b, hydrogenation of a dehydrogenated 2.5LiH + Si mixture does exhibit uptake of 4.9 wt % hydrogen. An initial mixture of 4LiH + Si was initially chosen because a silicide with the approximate composition of Li_4Si is a known phase, and this composition, if formed, would have yielded 6.6 wt % hydrogen. The data in Figure 1, together with the vacuum dehydrogenation, represent

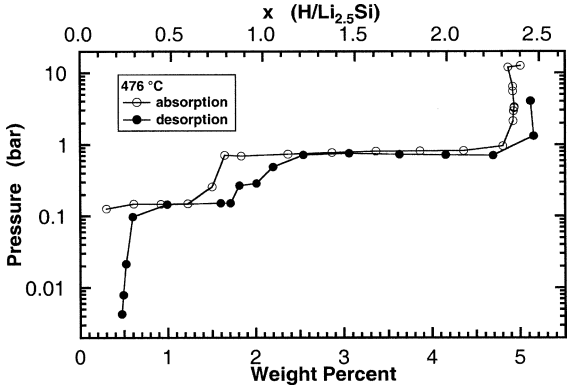

Figure 2. Absorption/desorption isotherms for milled 2.5LiH + Si mixture at 476 °C. Data were obtained by dehydrogenating the initial mixture under vacuum at 450 °C. Two flat plateaus are observed that correspond to transformations between known stoichiometric phases of Li silicides. The lower plateau, between ~0.5 and 1.5 wt % hydrogen, corresponds to the transformation of $Li_{2.35}Si$ to $Li_{1.71}Si$ ($Li_{12}Si_7$). Formation of $Li_{1.71}Si$ is complete at $x = 0.79$. The upper plateau, between 2.5 and 5.0 wt %, corresponds overall to the transformation of $Li_{1.71}Si$ to Si, although several intermediate composition silicides also form.

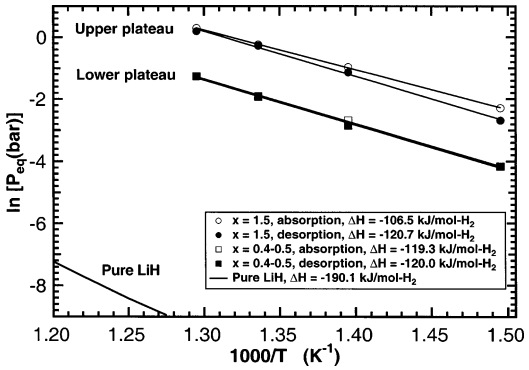

Figure 3. Van't Hoff plots for the lower ($x = 0.4-0.5$) and upper ($x = 1.5$) plateaus determined from the isotherms at 400−500 °C and, for comparison, pure LiH from ref 31. Addition of Si increases the equilibrium pressure by $>10^4$ times while lowering the dehydrogenation enthalpy from 190 to 120 kJ/mol H_2.

one hydrogen recovery and storage cycle. Three such cycles were performed with nearly identical kinetics; no degradation was observed.

To characterize the equilibrium behavior of the LiH/Si system, isotherms were measured for a 2.5LiH + Si mixture. A complete absorption/desorption isotherm at 476 °C is shown in Figure 2. The capacity is 5 wt % as expected for the 2.5LiH + Si mixture. Two distinct flat plateaus are observed. The first plateau occurs from 0.5 to 1.5 wt % at a pressure of 0.15 bar. The second plateau occurs between 2.5 and 5.0 wt % at a pressure of 0.74 bar. Between the two plateaus there is a transition region that may contain additional plateaus that are not resolved in the present measurements. The pressures of the plateaus are reversible, although there is hysteresis in the transition region.

Isotherms were also measured at 396, 444, and 499 °C. Qualitatively, these isotherms (not shown) are similar to that obtained at 476 °C, with two plateaus observed over the whole range of temperatures. The variation in the plateau pressures measured at $x = 0.4-0.5$ H/$Li_{2.5}Si$ and $x = 1.5$ H/$Li_{2.5}Si$ are shown in van't Hoff plots in Figure 3. The enthalpy for dehydrogenation for both plateaus is 120 kJ/mol H_2. In contrast, the equilibrium hydrogen pressure for LiH measured from 500 to 560 °C[31] is $>10^4$ times lower with an enthalpy of 190 kJ/mol H_2.

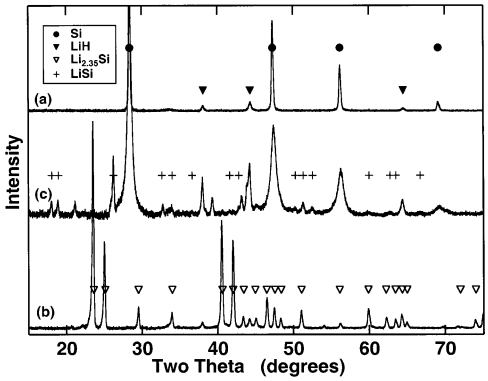

Figure 4. X-ray diffraction patterns from 4LiH + Si after milling, dehydrogenation, and rehydrogenation. Curve a, after 1 h milling is a physical mixture of Si and LiH. After vacuum dehydrogenation, curve b, $Li_{2.35}Si$ is the predominate phase, although some LiH is still detectable. Curve c, displayed on an expanded scale, shows that after rehydrogenation Si and LiH reform with broadened peaks. A small amount of LiSi is also present. The unmarked peaks in curve c correspond to an orthorhombic phase that does not match any of the known Li silicide compounds. Symbols show the location of major peaks for Si, LiH, $Li_{2.35}Si$, and LiSi from ICDD cards 89−2749, 89−4072, 89−6178, and 87−2075, respectively.

X-ray diffraction patterns from the milled reactants and the products after dehydrogenation and rehydrogenation are shown in Figure 4. The milled reactants are a physical mixture of Si and LiH. No new phases appear to have formed. After vacuum dehydrogenation some LiH remains, but the Si is entirely reacted. The main component is lithium silicide with a stoichiometry of $Li_{2.35}Si$. Upon rehydrogenation Si and LiH are formed, demonstrating that Si is not incorporated in a hydride phase. Compared to the as-milled mixture, after rehydrogenation the peaks for both Si and LiH are broad, suggesting that the crystallite size is small. In addition to Si and LiH, small amounts of the LiSi intermetallic are detectable, presumably because of incomplete rehydrogenation. X-ray diffraction measurements were also performed on several partially hydrogenated samples (data not shown). At $x = 0.77$, nearly pure $Li_{12}Si_7$, equivalent to $Li_{1.71}Si$, was identified. Given the overall stoichiometry of $Li_{2.5}Si$, $Li_{1.71}Si$ would be expected to occur at $x = 0.79$, i.e., a composition of $0.79LiH + Li_{1.71}Si$. At $x = 1.4$, Si and LiH were evident in addition to what appeared to be a pure orthorhombic phase. The diffraction pattern for this phase did not match the pattern of any known Li silicide compounds, although given the degree of hydrogenation the composition should be approximately LiSi. Some of this phase remains after rehydrogenation as shown in Figure 4. Work is continuing to characterize all the phases that form in the LiH/Si system.

Dehydrogenation of MgH_2 and a $2MgH_2 + Si$ mixture both milled identically are shown in Figure 5. In this case, the hydrogen pressure, rather than the wt % desorbed, is shown versus time. For pure MgH_2, desorption begins at approximately 295 °C, and a constant, equilibrium pressure of 1.65 bar was attained at 300 °C. This pressure is similar to the 1.83 bar that was measured previously.[15] The occurrence of equilibrium was checked by evacuating the desorbed hydrogen and then allowing desorption to continue. For the $2MgH_2 + Si$ mixture, desorption also begins at 295 °C; however, hydrogen evolution did not stop at the equilibrium value for pure MgH_2 but rather continued to increase until the temperature was lowered at 5.4 h. At 300 °C, the equilibrium pressure is, therefore, >7.5 bar, which is at least a factor of 4 larger than the pressure for pure MgH_2. The amount of hydrogen desorbed in the experiment

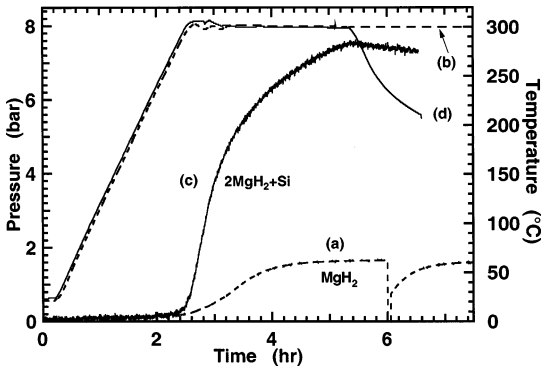

Figure 5. Hydrogen desorption from milled MgH_2 and $2MgH_2 + Si$. Curves a and b show pressure and temperature, respectively, for milled MgH_2 heated to 300 °C at 2 °C/min. At 300 °C, the pressure equilibrates at 1.65 bar. Evacuating the desorbed hydrogen, drop at 6 h, and then allowing desorption to continue demonstrates equilibrium. Curves c and d show the temperature and pressure, respectively, for a milled mixture of $2MgH_2 + Si$. In this case, the pressure does not equilibrate but continues to rise to >7.5 bar. In contrast to pure MgH_2, the stability of Mg_2Si that forms upon dehydrogenation drives the reaction to completion. The slight decline in pressure as the sample is cooled (at 5.4 h) is accounted for by gas cooling.

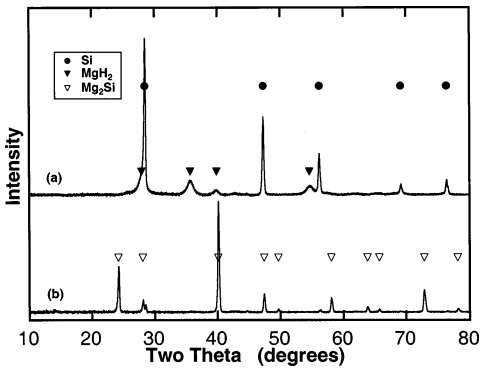

Figure 6. X-ray diffraction patterns from a $2MgH_2 + Si$ mixture after milling and after dehydrogenation at 400 °C. Curve a, after milling, is a physical mixture of MgH_2 and Si. After dehydrogenation, curve b, Mg_2Si is formed with a small amount of residual Si. Symbols show location of major peaks for Si, MgH_2, and Mg_2Si from ICDD cards 89−2749, 74−0934, and 65−2988, respectively.

shown in Figure 5 is 3.7 wt %, although desorption was still continuing when the sample was cooled. Heating to 400 °C yielded 4.3 wt %. In this case, the amount of recovered hydrogen appears to be kinetically limited by buildup of the Mg_2Si reaction product.

X-ray diffraction patterns from a milled mixture of $2MgH_2 + Si$ and a mixture dehydrogenated at 400 °C are shown in Figure 6. After milling, a physical mixture of MgH_2 and Si is observed. After dehydrogenation, Mg_2Si is the predominant phase, with a small amount of residual Si. The identity of the Mg_2Si phase was also indicated by its characteristic dark blue color.

Attempts at directly rehydrogenating a dehydrogenated $2MgH_2 + Si$ mixture using 100 bar hydrogen were unsuccessful. The difficulties in hydrogenation may be due to kinetic limitations. Rehydrogenation was attempted at temperatures as low as 150 °C for times up to 20 h. Addition of 5 atomic % Ti as a catalyst lowered the temperature for the onset of dehydrogenation from 295 to 210 °C, but rehydrogenation was still not observed. An uptake of 0.8 wt % hydrogen was achieved by milling pure Mg_2Si in 50 bar of hydrogen for 48 h. In this case, mechanical activation may have helped overcome the kinetic barriers to hydrogenation at low temperatures.

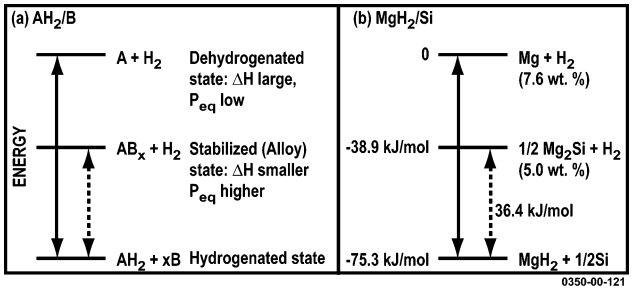

Figure 7. Energy diagrams illustrating hydride destabilization through alloy formation upon dehydrogenation. (a) Generic case for a binary hydride (AH_2) with an alloying element (B). (b) Example of MgH_2/Si. Alloy formation stabilizes the dehydrogenated state. The hydrogenated state enthalpy does not change. Thus, the enthalpy for dehydrogenation of the pure hydride (solid arrows) is reduced (dotted arrows). For MgH_2/Si, the stability of Mg_2Si reduces the standard enthalpy from zero (pure Mg + H_2) to −38.9 kJ/mol ($1/2Mg_2Si + H_2$), and thereby, the dehydrogenation enthalpy is reduced from 75.3 to 36.4 kJ/mol. Inclusion of Si also reduces the capacity from 7.6 to 5.0 wt % hydrogen.

4. Discussion

In general, for two components, hydride destabilization through alloy formation upon dehydrogenation involves the reaction

$$n\mathrm{AH}_x + \mathrm{mBH}_y \leftrightarrow \mathrm{A}_n\mathrm{B}_m + 1/2(nx + my)\mathrm{H}_2 \qquad (1)$$

where AH_x and BH_y are binary or more complex hydrides, and n and m are specified by the stoichiometry of the AB alloy. Two examples that we present here are the LiH/Si system with the reaction

$$4\mathrm{LiH} + \mathrm{Si} \leftrightarrow \mathrm{Li}_4\mathrm{Si} + 2\mathrm{H}_2 \qquad (2)$$

and the MgH_2/Si system with the reaction

$$2\mathrm{MgH}_2 + \mathrm{Si} \leftrightarrow \mathrm{Mg}_2\mathrm{Si} + 2\mathrm{H}_2 \qquad (3)$$

Both reactions 2 and 3 are instances of reaction 1 in which B is a nonhydriding species, i.e., $y = 0$. Because the formation of SiH_4 is endothermic, hydrogenation of Si is not expected under the conditions used in this work, and thus reactions 2 and 3 could be reversible. Because the Si does not hydrogenate, the Si addition reduces the gravimetric hydrogen density from that of the pure hydrides. For reactions 2 and 3, the hydrogen densities are 6.6 and 5.0 wt %, respectively.

The stability of the silicide (Li_4Si or Mg_2Si) is expected to destabilize the corresponding hydrides. For Mg_2Si, the standard enthalpy of formation is −77.8 kJ/mol.[32] Therefore, formation of Mg_2Si reduces the standard enthalpy of dehydrogenation of MgH_2 from 75.3 kJ/mol for pure MgH_2 to 36.4 kJ/mol for MgH_2 + 1/2Si. Figure 7 shows an energy diagram for the MgH_2/Si system, together with the generic case of a metal dihydride (AH_2) and a nonhydriding alloying element (B). Destabilization of the hydride increases the equilibrium pressure or, equivalently, reduces the temperature necessary for a particular equilibrium pressure. These thermodynamic data enable estimation of the equilibrium conditions. The data for Mg_2Si indicate that an equilibrium pressure of 1 bar hydrogen occurs at approximately 20 °C.[32] At 50 and 100 bar, the equilibrium temperatures are approximately 120 and 150 °C, respectively. These values imply that if reasonable reaction rates can be achieved at <150 °C, MgH_2/Si could be a practical hydrogen storage system.

The results presented here show that Si can significantly destabilize the strongly bound hydrides LiH and MgH_2. For the LiH/Si system, several Li silicide phases form upon dehydrogenation, which yield an equilibrium pressure of 1 bar at 490 °C and an enthalpy of dehydrogenation of 120 kJ/mol H_2. In contrast, pure LiH has an equilibrium pressure of 5×10^{-5} bar at 490 °C or, alternatively, 1 bar at 910 °C and an enthalpy of dehydrogenation of 190 kJ/mol H_2.[21,31] These destabilized equilibrium conditions remain outside the range needed for today's transportation applications but illustrate the large extent to which the thermodynamics can be altered.

The phase transformation behavior of the LiH/Si system, as shown in Figure 2, results in two distinct flat plateaus in the isotherms. These plateaus likely represent sequential formation and decomposition of increasingly Li-poor silicide phases as hydrogenation proceeds. Ultimately pure Si and LiH phases are formed. The complementary X-ray diffraction measurements indicate that the phase sequence upon hydrogenation is $Li_{2.35}Si$, $Li_{1.71}Si$ ($Li_{12}Si_7$), and LiSi. Hydrogen appears to form only the LiH phase over the whole composition range. The flatness of the plateaus is due to several factors. These are: (a) the absorption and desorption of hydrogen occurs in only phase-separated LiH, (b) the LiH that does form is at or near stoichiometry, and (c) the LiH forms in the presence of pure Li silicides with discrete compositions. Thermodynamic activities of separate pure solid phases are nearly unity. Thus, the solid phase activities are constant, i.e., near unity, throughout the two-phase regions. This constancy requires similarly constant hydrogen activities (or pressures), which give flat plateaus. Destabilized multiple phase systems composed of stoichiometric compounds with little mutual solubility may, therefore, be good candidates for hydrogen storage systems in which flat isotherm plateaus are desirable.

Within the precision of the van't Hoff plots, both plateaus in the LiH/Si isotherms yield similar dehydrogenation enthalpies of approximately 120 kJ/mol H_2. However, the difference in plateau pressures is a clear and sensitive indication that there are energetic differences between the phase equilibria occurring on each plateau. With a simple model of the isotherm and tabulated thermodynamic data for LiH, H_2, and Si, the plateau pressures can be used to estimate free energies for the different Li silicide phases. We assume that the lower pressure plateau corresponds to equilibrium between $Li_{2.35}Si$ and $Li_{1.71}Si$ and that the higher pressure plateau corresponds to equilibrium between $Li_{1.71}Si$ and Si. The free-energy change at standard state (P = 1 bar) and temperature T, given by ΔG_T°, can be expressed in terms of the free energy for each component (G_T°). As an example, for the higher pressure plateau

$$\Delta G_T^\circ = G_T^\circ(\mathrm{Li}_{1.71}\mathrm{Si}) + 0.855G_T^\circ(\mathrm{H}_2) - 1.71G_T^\circ(\mathrm{LiH}) - G_T^\circ(\mathrm{Si})$$

In addition, because the plateau represents equilibrium, $\Delta G_T^\circ = -RT \ln K$, where R is the gas constant and K is the equilibrium constant. If the activities for all of the solid phases are unity, then $K = P^n$, where P is the plateau pressure and n is the appropriate stoichiometric coefficient. Using pressures of 0.74 and 0.15 bar (from Figure 2) and G_T° at 476 °C for LiH, H_2, and Si (from ref 32) yields $G_T^\circ(Li_{1.71}Si) = -123.5$ kJ/mol or −72.2 kJ/g atom Li and $G_T^\circ(Li_{2.35}Si) = -159.2$ kJ/mol or −67.7 kJ/g atom Li. As expected from the phase sequence in the isotherms, decreasing Li content stabilizes the silicide on a per Li atom basis and, consequently, yields a lower dehydrogenation enthalpy and a higher plateau pressure. Although not

tabulated in databases, the free energies of formation from the elements ΔG_f° for several Li silicide phases have been determined electrochemically.[33] At 477 °C, $\Delta G_f^\circ(Li_2Si) = -31.1$ kJ/g atom Li and $\Delta G_f^\circ(Li_{2.63}Si) = -29.8$ kJ/g atom Li were measured. These values are similar to $\Delta G_f^\circ(Li_{1.71}Si) = -30.6$ kJ/g atom Li and $\Delta G_f^\circ(Li_{2.35}Si) = -29.2$ kJ/g atom Li determined here from the G_T° values above using the expression

$$\Delta G_f^\circ(Li_nSi) = G_T^\circ(Li_nSi) - nG_T^\circ(Li) - G_T^\circ(Si)$$

Although the compositions differ, the same trend of increasing stability with decreasing Li content is observed. In addition, the differences in stability between the two pairs of phases are similar.

For the MgH_2/Si system, Mg_2Si forms upon dehydrogenation, and the equilibrium pressure is >7.5 bar at 300 °C. Thermodynamic calculations based on the energetics shown in Figure 7 indicate that the equilibrium pressure should actually be >1000 bar at 300 °C. Experimentally, the observed pressure was limited by the sample size and the desorption volume. Under moderate conditions, the calculations indicate equilibrium pressures of 1−100 bar at temperatures of 20−150 °C, respectively. These conditions indicate why rehydrogenation was not observed in the MgH_2/Si system. At temperatures >150 °C, pressures in excess of 100 bar are required for hydrogenation. At temperatures <150 °C, the kinetics are likely too slow for significant hydrogenation. Although the intrinsic diffusion coefficient for MgH_2 is known to be very low,[12] reasonable hydrogenation rates could be achieved by reducing particle sizes to decrease diffusion distances and by catalysis to reduce activation barriers and facilitate hydrogen dissociation. However, initial attempts with Ti as a potential catalyst did not result in measurable hydrogenation. The effects of other additives will be examined in future work.

As mentioned above, alloy formation has been used previously to destabilize metal hydrides, most notably MgH_2. However, the modifying elements have been predominately metals such as Ni, Fe, Al, or Cu. Destabilization has been achieved, but the effect has been relatively small, with an increase in equilibrium pressure of less than a factor of 10. Only relatively small changes have been achieved because either the stabilization was weak, for example Mg/Al, or alloy formation occurred in both the hydrogenated and dehydrogenated states, for example Mg_2Ni. If the stabilization is weak, then Figure 7 shows that the enthalpy for dehydrogenation will change only slightly. If alloy formation, i.e., stabilization, occurs in both hydrogenated and dehydrogenated states, then the effect largely cancels because only the difference in stabilization energy contributes to lowering the dehydrogenation enthalpy. In contrast, Si forms strongly bound compounds only in the dehydrogenated state. Therefore, the changes in thermodynamics are relatively large with increases in equilibrium pressures of more than a factor of 1000.

Similar to Si, Ge forms stable compounds with Mg and these compounds have been found to form upon dehydrogenation of MgH_2 + Ge mixtures.[34] However, the effect on equilibrium pressure has not been established. Although usually considered separate from reversible hydrides, production of hydrogen by hydride hydrolysis[35] is, broadly, an example of destabilization. With hydrolysis, destabilization is extreme, the oxides or hydroxides that form upon dehydrogenation are very stable, and consequently, the evolution of hydrogen becomes exothermic, thus rendering the reaction irreversible.

Beyond LiH and MgH_2, the approach used here can be applied generally. Other alloying elements with lower atomic weight or more desirable stoichiometries could increase the hydrogen storage density or further improve the equilibrium pressures. In addition to Si and Al, interesting possibilities include B, C, N, P, and S. Strongly bound complex hydrides with high hydrogen densities such as $LiBH_4$ might also be favorably altered. Replacing a nonhydriding alloying element, such as Si, with an appropriate hydride could enable destabilization without reducing storage densities. An interesting possibility occurs if, instead of stoichiometric compounds, A and B in reaction 1 form a continuous solid solution. In this case, the equilibrium may be tuned by varying *n* and *m*. Finally, the number of components need not be restricted to two; an arbitrary number may be used to achieve optimal performance.

5. Summary

Alloy formation with Si that occurs upon dehydrogenation has been shown to destabilize LiH and MgH_2. For the LiH/Si system, the equilibrium pressure at 490 °C is approximately 1 bar, which is $>10^4$ times the pressure for pure LiH. Van't Hoff plots obtained from isotherms measured at 400−500 °C yield an enthalpy for dehydrogenation of approximately 120 kJ/mol H_2. In contrast, the dehydrogenation enthalpy of pure LiH is approximately 190 kJ/mol H_2. The reversible capacity for a 2.5LiH + Si mixture is 5.0 wt %. For the MgH_2/Si system, Mg_2Si forms upon dehydrogenation. Experimentally, the equilibrium pressure at 300 °C is more than 7.5 bar, which is more than 4 times the pressure for pure MgH_2. Calculations using tabulated thermodynamic parameters predict an equilibrium pressure of 1 bar at approximately 20 °C and 100 bar at approximately 150 °C, which represent an increase of more than a factor of 1000 over the pressure for pure MgH_2. These conditions make the MgH_2/Si system, which has a capacity of 5.0 wt %, a candidate for practical hydrogen storage at reduced temperatures. However, thus far, the kinetics at 150 °C are too slow for direct hydrogenation. Overall, the results illustrate that the strategy of using alloying elements to form stable compounds or alloys upon dehydrogenation can be used to increase the equilibrium pressures of hydrogen-rich but strongly bound hydrides.

Acknowledgment. C.C.A. would like to acknowledge partial support for this work by DOE through Energy Efficiency and Renewable Energy Grant No. DE-FC36-01GO11090 and by the Chemical and Environmental Sciences Laboratory of General Motors Research and Development Center. This research was partially performed at the Jet Propulsion Laboratory, which is operated by the California Institute of Technology under contract with the U.S. National Aeronautics and Space Administration (NASA).

References and Notes

(1) Schlapbach, L.; Züttel, A. *Nature* **2001**, *414*, 353.

(2) Züttel, A. *Mater. Today* **2003**, *6*, 24.

(3) *National Hydrogen Energy Roadmap*; U.S. Department of Energy; 2002, p 17. http://www.eere.energy.gov/hydrogenandfuelcells/pdfs/hydrogen_posture_plan.pdf.

(4) *A Multiyear Plan for the Hydrogen R&D Program: Rationale, Structure, and Technology Roadmaps*; U.S. Department of Energy; 1999, p 32. http://www.eere.energy.gov/hydrogenandfuelcells/pdfs/bk28424.pdf.

(5) Bénard, P.; Chahine, R. *Langmuir* **2001**, *17*, 1950.

(6) Chahine, R.; Bose, T. K. *Int. J. Hydrogen Energy* **1994**, *19*, 161.

(7) Züttel, A.; Orimo, S. *MRS Bull.* **2002**, *27*, 705.

(8) Hirscher, M.; Becher, M.; Haluska, M.; Dettlaff-Weglikowska, U.; Quintel, A.; Duesberg, G. S.; Choi, Y-M.; Downes, P.; Hulman, M.; Roth, S.; Stepanek, I.; Bernier, P. *Appl. Phys. A* **2001**, *72*, 129.

(9) Ye, Y.; Ahn, C. C.; Witham, C.; Fultz, B.; Liu, J.; Rinzler, A. G.; Colbert, D.; Smith, K. A.; Smith, K. A.; Smalley, R. E. *Appl. Phys. Lett.* **1999**, *74*, 2307.

(10) Dillon, A. C.; Jones, K. M.; Bekkedahl, T. A.; Kiang, C. H.; Bethune, D. S.; Heben, M. J. *Nature* **1997**, *386*, 377.

(11) Dillon, A. C.; Gilbert, K. E. H.; Parilla, P. A.; Alleman, J. L.; Hornyak, G. L.; Jones, K. M.; Heben, M. J. "Hydrogen storage in carbon single-wall nanotubes." In *Proceedings of the 2002 U.S. DOE Hydrogen Program Review*; NREL/CP-610-32405; 2002. http://www.eere.energy.gov/hydrogenandfuelcells/annual_review2002.html#Storage.

(12) Bowman, R. C., Jr.; Fultz, B. *MRS Bull.* **2002**, *27*, 688.

(13) Sandrock, G. *J. Alloys Compd*. **1999**, *293*−*295*, 877.

(14) Sandrock, G.; Thomas, G. *Appl Phys. A* **2001**, *72*, 153.

(15) IEA/DOE/SNL Hydride Databases available at Hydride Information Center, Sandia National Laboratories Home Page. http://hydpark.ca.sandia.gov/.

(16) Bogdanovíc, B.; Sandrock, G. *MRS Bull.* **2002**, *27*, 712.

(17) Jensen, C. M.; Gross, K. J. *Appl Phys. A* **2001**, *72*, 213.

(18) Ritter, J. A.; Ebner, A. D.; Wang, J.; Zidan, R. *Mater. Today* **2003**, *6*, 18.

(19) Chen, P.; Xiong, Z.; Luo, J.; Lin, J.; Tan, K. L. *Nature* **2002**, *420*, 302.

(20) Chen, P.; Xiong, Z.; Luo, J.; Lin, J.; Tan, K. L. *J. Phys. Chem. B* **2003**, *107*, 10967.

(21) Sangster, J.; Pelton, A. D. In *Phase Diagrams of Binary Hydrogen Alloys*; Manchester, F. D., Ed.; ASM International: Materials Park, OH, 2000; p 74.

(22) Huot, J.; Liang, G.; Schulz, R. *Appl. Phys. A* **2001**, *72*, 187.

(23) Schwarz, R. B. *MRS Bull.* **1999**, *24*, 40.

(24) Bouaricha, S.; Dodelet, J.-P.; Guay, D.; Huot, J.; Schulz, R. *J. Mater. Res.* **2001**, *16*, 2893.

(25) Liang, G.; Huot, J.; Boily, S.; Van Neste, A.; Schulz, R. *J. Alloy Compd*. **1999**, *292*, 247.

(26) Reilly, J. J.; Wisall R. H. *Inorg. Chem.* **1968**, *7*, 2254.

(27) Reilly, J. J.; Wisall R. H. *Inorg. Chem.* **1967**, *6*, 2220.

(28) Zaluska, A.; Zaluski, L.; Ström-Olsen, J. O. *Appl. Phys. A* **2001**, *72*, 157.

(29) Wiswall, R. H. In *Hydrogen in Metals II*; Alefeld, G., Volkl, J., Eds.; Springer-Verlag: Berlin, 1978; Vol. 29, p 201.

(30) Orimo, S.; Fujii, H. *Appl. Phys. A* **2001**, *72*, 167.

(31) Veleckis, E. *J. Nucl. Mater*. **1979**, *79*, 20.

(32) Estimates of thermodynamic parameters and equilibrium pressures were made using *Outokumpu HSC Chemistry* for Windows, version 4.0; ChemSW, Inc. 1999.

(33) Sharma, R. A.; Seefurth, R. N. *J. Electrochem. Soc.* **1976**, *123*, 1763

(34) Gennari, F. C.; Castro, F. J.; Urretavizcaya, G.; Meyer, G. *J. Alloy Compd*. **2002**, *334*, 277.

(35) Kong, V. C. Y.; Foulkes, F. R.; Kirk, D. W.; Hinatsu, J. T. *Int. J. Hydrogen Energy* **1999**, *24*, 663.